Scaling of membrane-type locally resonant acoustic metamaterial arrays

Christina J. Naify[a)]
Department of Materials Science, University of Southern California, 3651 Watt Way, VHE 402, Los Angeles, California 90089

Chia-Ming Chang and Geoffrey McKnight
HRL Laboratories, 3011 Malibu Canyon Road, Malibu, California 90265

Steven R. Nutt
Department of Materials Science, University of Southern California, 3651 Watt Way, VHE 602, Los Angeles, California 90089

(Received 30 November 2011; revised 11 May 2012; accepted 31 May 2012)

Metamaterials have emerged as promising solutions for manipulation of sound waves in a variety of applications. Locally resonant acoustic materials (LRAM) decrease sound transmission by 500% over acoustic mass law predictions at peak transmission loss (TL) frequencies with minimal added mass, making them appealing for weight-critical applications such as aerospace structures. In this study, potential issues associated with scale-up of the structure are addressed. TL of single-celled and multi-celled LRAM was measured using an impedance tube setup with systematic variation in geometric parameters to understand the effects of each parameter on acoustic response. Finite element analysis was performed to predict TL as a function of frequency for structures with varying complexity, including stacked structures and multi-celled arrays. Dynamic response of the array structures under discrete frequency excitation was investigated using laser vibrometry to verify negative dynamic mass behavior. © *2012 Acoustical Society of America*. [http://dx.doi.org/10.1121/1.4744941]

PACS number(s): 43.40.Qi, 43.40.Dx [ANN] Pages: 2784–2792

I. INTRODUCTION

Construction of aerospace structures relies increasingly on composite materials designed to provide increased strength-to-weight ratios compared to traditional metal-based constructions.[1–4] Although composite structures are ideal for mechanical performance, acoustic transmission loss performance (noise mitigation) is compromised, resulting in the need for lightweight acoustic treatments. Traditional acoustic isolation approaches employ combinations of mass, acoustic absorption, and sealing, which are effective at lower frequencies with sufficient mass, but are ineffective at low frequencies because of mass law-dominated performance.[5] Several approaches have been considered to improve acoustic insulation without increased weight penalty. These have included addition of mass inclusions to foam materials,[6] impedance mismatch of gas layers,[7] and the use of micro-perforated panels.[8] These approaches have shown varying degrees of improvement in sound insulation, although they have provided minimal increase in transmission loss (TL) ($<$20 dB) at low frequencies ($<$1000 Hz).

Metamaterials derive their properties from structure rather than composition, and were initially proposed by Veselago[9] for manipulation of electromagnetic (EM) waves. Similarities between EM and acoustic waves led to the development of acoustic metamaterials with negative dynamic mass and modulus.[10–15] A broad range of applications for these structures have been proposed, such as cloaking,[16–18] diodes,[19] and sound insulation.[20,21] Locally resonant acoustic materials with negative dynamic mass density have been shown to demonstrate significant increase (5×) in TL over mass law predictions for a narrow band (100 Hz) at low frequencies (100–1000 Hz).[14,22–24] In recent work, the peak TL frequency was tuned to specific values by varying the membrane properties and mass. Investigation of single-celled structures included measured and predicted TL response, characterization of mode shapes,[15,25] and experimental verification of negative dynamic mass at the peak TL frequency.[15] The variation in mass magnitude across the array locally resonant acoustic materials (LRAM) and the effect of support frame compliance was evaluated, and demonstrated that decreased compliance resulted in decreased TL peak bandwidth.[26]

In the present work, a more complete parametric analysis is presented to guide the scale-up of the LRAM structure from a single cell to multi-celled array and to explore issues and effects associated with scale-up. Previous studies focused on characterization of single-celled structures, to understand the underlying physical phenomena,[15] and small-scale (four-celled) arrays, to understand the effects of multiple cells.[26]

In this study, some of the issues encountered in scale-up of the structure are addressed, including multi-cell dynamics, variation in cell size, and broadening of the TL peak to increase the sound insulation bandwidth. TL of single-celled structures is measured for variations in the mass magnitude and membrane radius using an impedance tube setup. The

[a)]Author to whom correspondence should be addressed. Electronic mail: christina.naify@gmail.com

measured TL is compared to the results of acoustic-structural finite element analysis (FEA) modeling to understand the role of each geometric parameter on the acoustic performance. TL of stacked, single-celled structures is also evaluated using both experimental and FEA techniques with variation in mass distribution between each stacked layer, and variation in stacking distance. Depending on the mass distribution between each layer, increased TL or multiple TL peaks was achieved.

Four-celled coupons were also constructed and analyzed to better understand the response of array structures. TL behavior was measured for multiple configurations with different magnitudes of mass distributed across each of the cell membranes in the array. The frame stiffness was also varied to determine the effect of the frame vibration on LRAM performance. The measured TL of the multi-celled structure was compared to TL behavior predicted by FEA to understand the effect of increasing the number of cells. Finally, multiple four-celled panels were stacked in series to create a structure with increased TL bandwidth. Dynamic response of array structures was evaluated to determine the phase relationship between cells and verify negative dynamic mass of the array.

Section II of the study provides details of both the structure fabrication and characterization. Results are presented in Sec. III for both the single-cell and multi-celled structures. The results are then discussed in Sec. IV and the implications of the research are considered in Sec. V.

II. METHODS

A. Sample fabrication

Membrane-type LRAM structures were constructed of a thin, tensioned membrane, a centrally located mass, and a support frame [Fig. 1(a)]. Two sample types were constructed—a circular single-cell sample with diameter of 24 mm, and a four-cell array with each cell 27.4 mm across. The four-celled array structure [Fig. 1(b)] was mounted in a tube adaptor constructed of 10 mm thick steel with a diameter of 100 mm. Mass was added to the membranes by bonding small metal disks (0.08 g, 3 mm diameter) to the center of each cell. For low-frequency cells, a soft silicone rubber was used for the membranes, while for higher frequencies, a stiff thermoplastic, polyetherimide (PEI), was used.

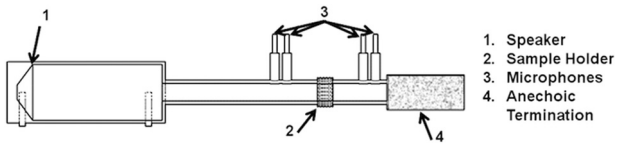

FIG. 2. Schematic of small-diameter impedance tube showing locations of speaker, microphones, and sample.

The multi-celled arrays were constructed by stretching a large single membrane over a support frame [Fig. 1(b)]. Mass was bonded to the center of each cell in the array. The array frames had square cells with a side length of 27.4 mm. Dimensions of the frame (2 mm wide) resulted in a center-to-center cell distance of 29.4 mm. Membranes were bonded to the support structure using a heat-activated adhesive. During the curing process, the difference in thermal expansion coefficient between the membrane and support was exploited to introduce tension into the membrane. Tension was measured by adding mass to the center of the structure and measuring the out-of-plane displacement of the membrane as a function of mass magnitude (for further details, see Ref. 7).

The support structure for the single-cell structure was constructed of a quasi-isotropic composite (glass fiber and epoxy), while the support structure for the array structures was aluminum. The thickness of all of the frame materials was 1 mm.

B. Characterization

Normal incidence sound transmission measurements for the single-cell and four-celled array structures were conducted using an impedance tube (Brüel and Kjær model 4206, ASTM E2611-09).[27] Figure 2 shows a schematic of the impedance tube used for measuring TL of the 29 mm diameter circular samples over a frequency range of 100 Hz–6.4 kHz. The TL of the four-celled array was measured using a large-diameter impedance tube (schematic not shown, frequency

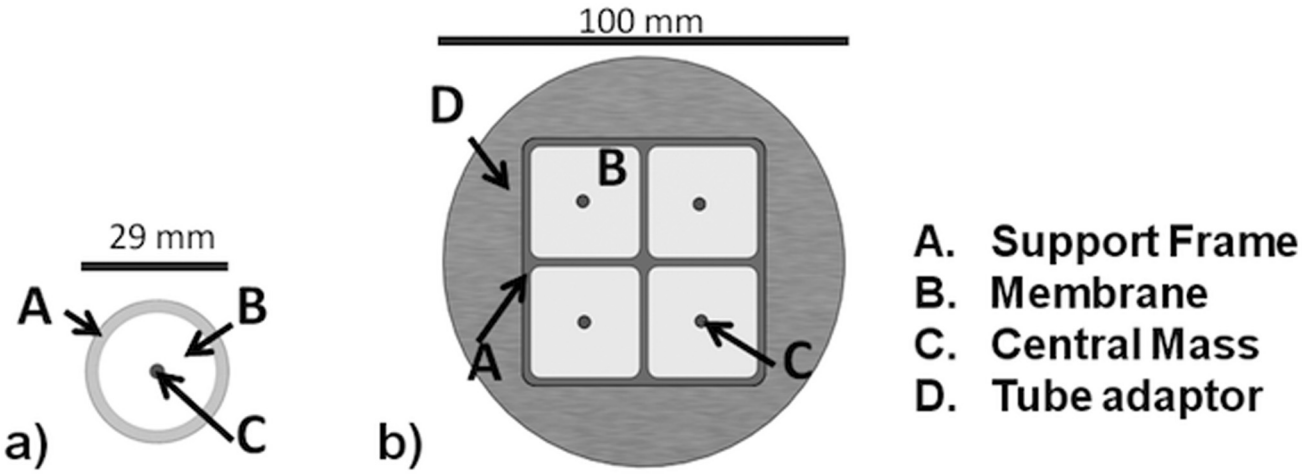

FIG. 1. Schematics of samples. (a) Single-cell circular sample, (b) four-celled array structure; support structure (A), membrane (B), central mass (C), and tube adaptor (D).

range 50 Hz–2 kHz). All of the samples were mounted in the tube with a clamped boundary condition and excited using a broadband, plane wave sound source. Two microphones were positioned upstream of the sample to measure the incident sound pressure level, while two additional microphones were situated downstream of the sample to measure the transmitted sound pressure level. An anechoic termination (in the form of a foam plug) on the receiver side of the sample prevented transmitted sound from being reflected back to the sample. The TL of the structure was calculated using a transfer matrix method (PULSE software, Brüel and Kjær).

III. RESULTS

A. Single cell

Transmission loss of the circular, single-celled structures was evaluated for various mass magnitudes and mass diameters. The measured TL profile of the structure with variation in mass magnitude is shown in Fig. 3(a). As the magnitude of mass attached to the center of the membrane was increased, the TL peak frequency decreased, while the magnitude of the TL peak increased. Similar trends were observed for the low-frequency resonance, while the high-frequency resonance frequency was unchanged. Increase in the magnitude of mass by a factor of 3 increased the TL peak magnitude by 11 dB. Figure 3(b) shows the measured TL with increase in mass radius (membrane radius and material and mass magnitude were constant for each mass radius). As the mass radius was increased from 1.5 to 5 mm the TL peak and resonance frequencies increased. The TL peak frequency increased from ~700 Hz to ~1.1 kHz. The magnitude of the TL peak, however, remained constant with variation in mass radius.

Figures 4(c) and 4(d) show TL curves predicted using FEA software (COMSOL MULTIPHYSICS), and these can be compared with the experimental results in Figs. 4(a) and 4(b). The acoustic-structure interaction model for the circular single cell surrounding by air was constructed using axial symmetry with the same dimensions as the experimental impedance tube setup. The physical parameters, including air density (1.29 kg/m^3) and speed (340 m/s) at room temperature, along with material properties, were assigned to each component in the model. In our calculations, the mass density, Young's modulus, and the Poisson's ratio for the PEI membrane were 1200 kg/m^3, 3.6×10^9 Pa, and 0.36, respectively, while mass density, Young's modulus, and Poisson's ratio for the central mass are 7738 kg/m^3, 1.7×10^{11} Pa, and 0.3, respectively. Material damping was not included because the PEI film has a low damping factor ($\tan \delta = 0.01$), and membrane damping had a negligible contribution to sound reflection in the current configuration. To confirm this assumption, simulations were performed using a material damping factor of 0.01, and these showed behavior nearly identical to the undamped model. For strong damping ($\tan \delta = 0.5$), the model showed similar critical frequencies in the TL prediction but with reduced TL peaks. The measured membrane tension was also applied as initial stresses in the radial and tangential directions of the membrane. To closely simulate the membrane dynamic

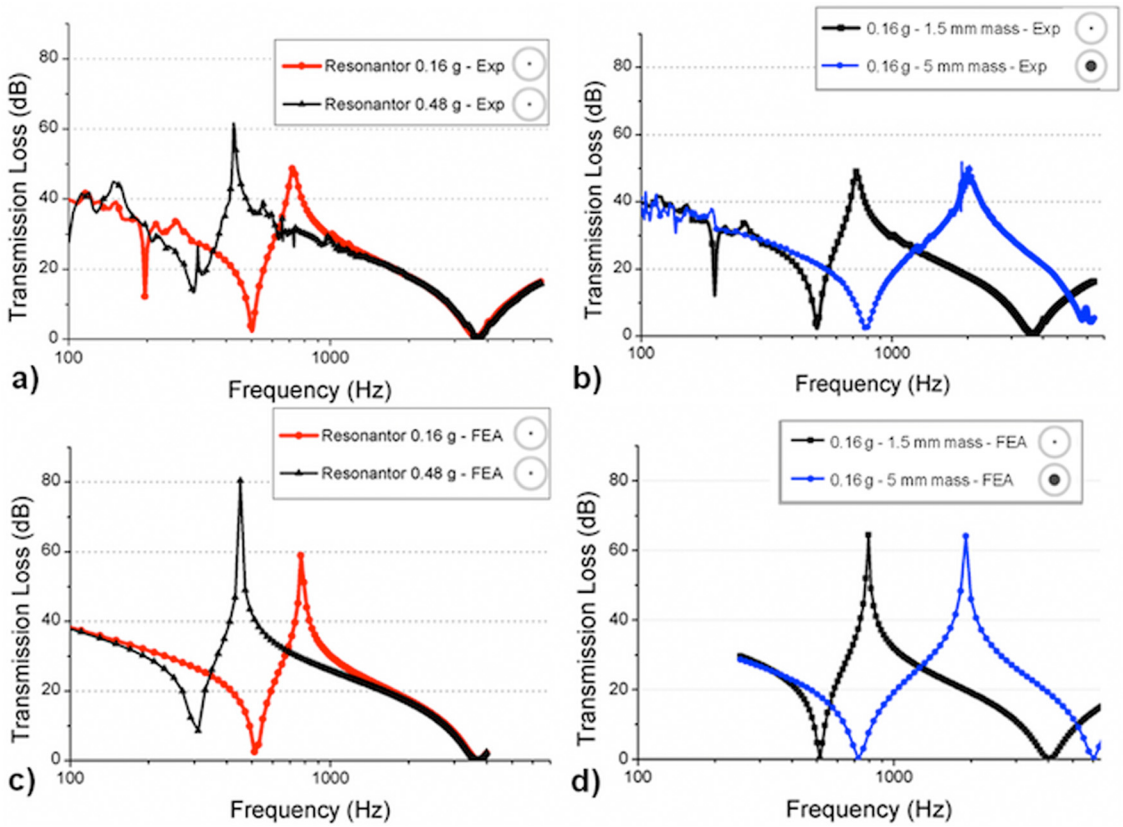

FIG. 3. (Color online) TL of single-cell circular samples. (a) Measured TL, mass magnitude variation, (b) measured TL, mass radius variation, (c) FEA-predicted TL, mass magnitude variation, (d) FEA-predicted TL, mass radius variation.

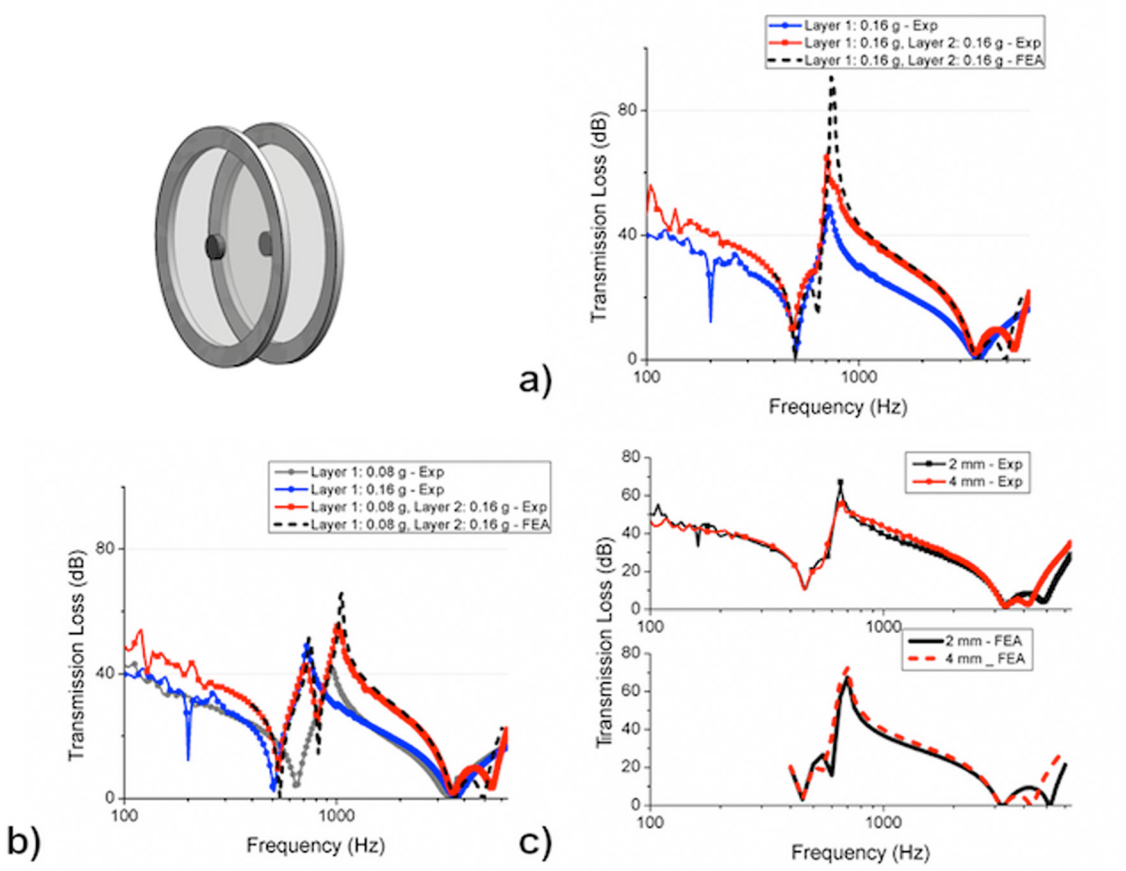

FIG. 4. (Color online) Measured and FEA-predicted TL of single-cell LRAM structures showing (a) identical stacked structures with 0.16 g central mass magnitude (dashed line–FEA prediction), (b) non-identical structures with 0.08 g on layer 1 and 0.16 g on layer 2, (c) measured (top) and FEA-predicted (bottom) TL response of stacked identical structures with variation in stacking distance.

response as a function of film thickness, a nonlinear solver and a fine triangle mesh approach with 10 466 elements and 60 544 degree of freedom was used to ensure at least four elements across the membrane thickness. The membrane edge was assigned a fixed boundary condition, and the differential sound pressure level applied to the boundary of the model was 1 Pa. By calculating the incident and transmitted acoustic power, the TL curves in decibels were plotted as functions of frequency. As shown in Figs. 4(c) and 4(d), the FEA predictions differed from the measured results by less than 10%.

Transmission loss for structures stacked in series was also measured using the impedance tube setup. Identical samples were mounted in the impedance tube and separated by a 3 mm wide spacer. The samples were mounted with a clamped boundary condition. A schematic showing the orientation of the stacked structures is shown in Fig. 4 (upper left corner). The TL measured for stacked samples with identical mass magnitude (0.16 g/cell) is shown in Fig. 4(a) along with the measured TL for a single sample with 0.16 g/cell. The magnitude of the TL peak for the stacked samples was 64 dB, while the magnitude of a single sample was 47 dB. The first resonance, second resonance, and TL peak frequencies for the configuration with stacked samples were within 3% of the frequencies for the single layer configuration. The overall TL for the stacked configurations, however, was ~10 dB higher than that of the single cell. The stacked configuration produced a resonance frequency at 5 kHz, as well as the same high-frequency resonance as the single sample (~3.5 kHz).

The TL was measured for non-identical stacked samples in which the first layer (closest to the incident sound field) featured 0.08 g/cell, while the second layer (closest to the tube termination) featured 0.16 g/cell. The TL measured for each individual layer (0.08 and 0.16 g/cell) as well as the TL measured for the stacked configuration are shown in Fig. 4(b). The TL profile for the stacked configuration consisted of two TL peaks with each peak corresponding to the TL peaks of the individual panels. The overall TL for the stacked configuration was ~10 dB higher than that of the individual panels. The high-frequency resonance for the stacked configuration was ~3.5 kHz with an additional resonance occurring at ~5 kHz, similar to observations for the identical panel configurations.

The effect of panel separation on TL was investigated by varying the sample spacing from 2 to 4 mm. Each of the samples had identical membrane properties and a mass magnitude of 0.16 g. Below 1 kHz, the stacking distance had negligible effect on the TL behavior of the stacked structures [see Fig. 4(c)]. Identical stacked structures with 0.16 g/cell showed a TL peak magnitude of 47 dB at a frequency of 696 Hz. Increasing the stacking distance to 4 mm resulted in an increase in the overall TL magnitude of 2–3 dB. As shown in Figs. 4(a) and 4(b), varying the mass magnitude did not affect the high-frequency resonance behavior. Decreasing

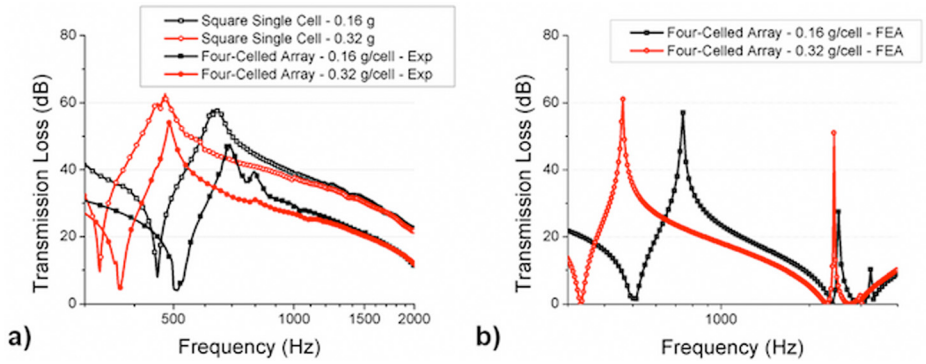

FIG. 5. (Color online) (a) Measured TL of four-celled array structure with increased mass magnitude (0.16 and 0.32 g/cell), as well as measured TL of square, single-celled structure with mass magnitude of 0.16 and 0.32 g, (b) FEA predictions of TL for four-celled array with increased mass magnitude (0.16 and 0.32 g/cell).

the stacking distance between the structures resulted in an increase in the third resonance frequency from 4.2 to 5.3 kHz.

FEA was used to predict the TL of the stacked structures with varying mass distributions and stacking distances. The predicted TL profiles for identical and non-identical configurations, and for variation in stacking distance, are shown in Figs. 4(a)–4(c). The peak TL frequencies of the FEA prediction were within 4% of the measured frequencies, while the first resonance frequencies were within 2%. The analysis was accurate in predicting the overall TL magnitude, although the predicted magnitude at the TL peak was larger than the measured magnitude. The measured results and the FEA results were symmetric—reversing the stacking order of the samples did not change the TL of the configuration.

B. Four-celled array

The TL measured for the four-celled array with variation in mass magnitude across the cells is shown in Fig. 5(a). Additionally, TL was measured for a square, single-celled structure (schematic not shown).[26] The square single cell had a side length of 27.4 mm with membrane properties identical to those used in the four-celled array. The single-celled square sample was mounted in a tube adaptor similar to that used for the array (10 mm thick, diameter of 100 mm), and TL was measured in the large-diameter impedance tube. The measured TL for the square single-cell sample with 0.16 and 0.32 g mass magnitude is shown in Fig. 5(a), as well as the TL of the array structure with 0.16 and 0.32 g/cell.

Increasing the central mass magnitude resulted in both a decrease in peak TL frequency and an increase in TL peak magnitude, much like the circular single-cell structure. The four-celled array structure with uniform mass distribution displayed a single TL peak and a single low-frequency resonance, with frequencies similar to those of the square single cell. The magnitude of the TL for the square single cell, however, was ~10 dB greater than that of the array structure, with peak TL and resonance frequencies about 10% lower than those measured for the array.

FEA-predicted TL for the four-celled array structure with variation in central mass magnitude is shown in Fig. 5(b). The FEA model used a two-dimensional shell structure to facilitate calculation intensity. As with the single-cell model, the FEA did not include damping in the membrane material and used an incident pressure of 1 Pa. Predicted values of resonance and TL peak frequencies were within 10% of the measured values. Table I shows measured first resonance and TL peak frequencies for the square single cell and four-celled array, as well as FEA-predicted peak and resonance frequencies for the four-celled array. The differences between the measured and FEA-predicted results (expressed as percent) for the four-celled array structure are included in parentheses.

Although high-frequency resonance results were not measured due to the frequency cutoff of the impedance tube (~2 kHz), predicted results are reported in Table I. The FEA predictions for the four-celled array structure shows an anti-resonance occurring at ~2.3 kHz, the membrane resonance occurring at ~3 kHz, and an additional resonance occurring at ~2 kHz. The high-frequency behavior of the structure was negligibly affected by the change in mass magnitude, the most significant change being an increase in anti-resonance magnitude corresponding to the mass increase.

FEA was also used to predict the TL response for a four-celled array structure with variations in frame stiffness.[26] The membrane materials were the same as those used in the experimentally evaluated four-celled array. The size of each cell in the array was 27.4 mm on each side. Figure 6

TABLE I. Resonance and TL peak frequencies of square single-celled and four-celled arrays. Percent difference between the experimentally obtained and predicted frequency values for the four-celled array are included in parentheses.

Frequency	Experimental—square single cell	Experimental—four-celled array	FEA—four-celled array
First resonance—0.16 g (Hz)	455	504	501 (−0.59)
TL peak—0.16 g (Hz)	645	692	744 (7.51)
Second resonance—0.16 g (Hz)	—	—	2398
First resonance—0.32 g (Hz)	327	368	331 (−10.05)
TL peak—0.32 g (Hz)	475	488	461 (−5.53)
Second resonance—0.32 g (Hz)	—	—	2398

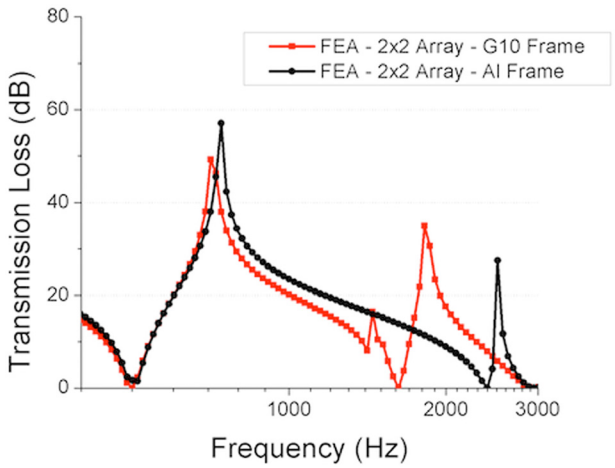

FIG. 6. (Color online) FEA-predicted TL of 2 × 2 array structure with varying frame compliance (0.16 g/cell).

shows the predicted TL of the four-celled structure with variation in frame compliance.

The two frame materials examined were aluminum and a glass-fiber, epoxy composite (G10). The average modulii of these materials was 75 and 17.5 GPa, respectively. The TL peak frequency was predicted to be ~700 Hz, similar to that of the square, single-celled sample with identical mass magnitude. However, the TL peak frequency bandwidth of the structure with a composite frame was less than the frequency bandwidth of the aluminum-frame four-celled structure, with bandwidth defined as the frequency range between the two resonance frequencies.

The transmission loss of array panels stacked in series was measured using the same impedance tube setup. Identical tube adaptors and membrane materials were used for each array panel. Two configurations of mass magnitude were measured. The first configuration had identical panels, with equal mass magnitude on each cell of the array panels. The second configuration had non-identical panels with different mass magnitudes distributed across each array panel, and the stacked arrays were 10 mm apart in each case. Figure 7 (left) shows a schematic of the two panels arranged in series (tube adaptors omitted from schematic for simplification). Figure 7(a) shows the TL measured for a single panel with 0.16 g/cell as well as for stacked identical panels with 0.16 g/cell. The TL profile of the identical stacked panels [Fig. 7(a)] resulted in a single TL peak and a single low-frequency resonance, with the TL peak and resonance frequencies within 9% of the values measured for the single panel. The magnitude of the TL peak for the stacked panels, however, was up to 19 dB greater than the TL peak measured for the single panel.

Measured TL of non-identical panels stacked in series is shown in Fig. 7(b) along with the measured TL for each panel individually. The mass distribution on the panels was 0.16 g/cell on the first panel, and 0.32 g/cell on the second panel. Changing the stacking order of the panels, or the distance between the panels, did not affect the TL performance within the frequency range examined. The TL of the non-identical stacked panels exhibited a two-peak profile, with each of the TL peaks corresponding to the TL peaks of the individual panels. The mass law predicted TL for the stacked, non-identical panels was calculated using a composite mass law equation,[28–30] including the mass of the membrane, central mass, and frame material. The measured TL peak of the stacked panels was 40 dB greater than the mass law predicted TL at 750 Hz (TL peak frequency of the 0.16 g/cell configuration).

IV. DISCUSSION

Geometric variations to the single-celled LRAM structure altered the frequency of the TL peak. Increasing the mass magnitude or membrane radius decreased the TL peak frequency, and the mass resonance frequency.[15] In contrast, increasing the mass magnitude did not change the membrane resonance of the single-celled structure. Increasing the mass radius, however, resulted in an increase in membrane resonance frequency due to the associated decrease in effective membrane radius. The 11 dB increase in TL peak magnitude observed with increase in mass was attributed to the increase in overall mass of the structure. Increasing the mass radius did not result in a TL peak magnitude change because the overall mass of the structure remained constant. Utilization of FEA to predict TL behavior of the structures was accurate in predicting the resonance and peak TL frequencies to within 6% of measured values.

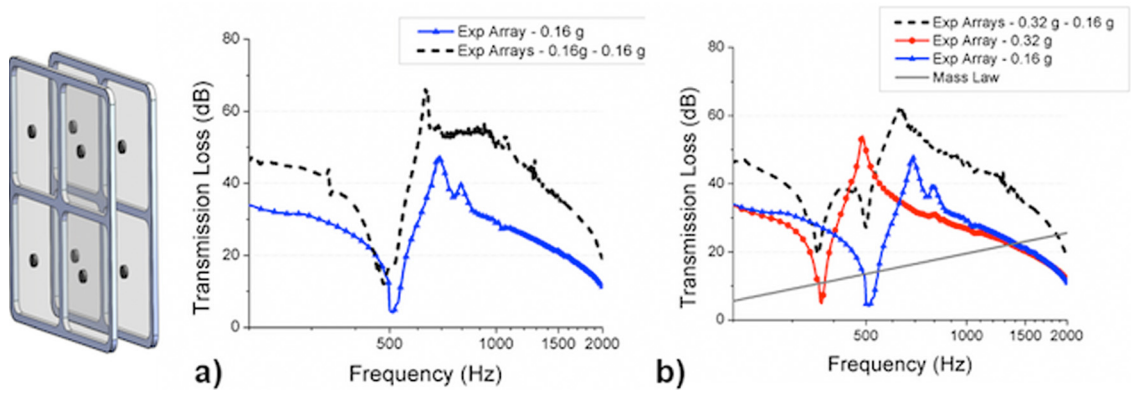

FIG. 7. (Color online) Measured TL of stacked array panels. Schematic (left) of panels stacked in series, (a) TL of identical panels with 0.16 g/cell, (b) TL of panels with 0.32 g/cell (layer 1) and 0.16 g/cell (layer 2) with predicted mass law TL.

The TL of stacked single-celled samples was also measured in the small diameter impedance tube. Stacking of identical samples resulted in a single TL peak profile with increased TL peak magnitude, as well as TL peak and resonance frequencies within 4% of those for the single cell. Non-identical structures (with different mass magnitudes) stacked in series resulted in a multi-peak TL profile. The TL peaks measured for the stacked structures were similar to those measured for each individual sample, with an overall increase in TL of about 10 dB measured for the stacked structure. The observed increase in overall TL of ~10 dB was attributed to the increased mass of the stacked structure over the single-layer structure, as well as the effect from the double-wall structure.[30]

FEA predictions of TL behavior of the stacked structures yielded values of TL peak and resonance frequencies within 4% of the measured values. FEA was accurate in predicting the overall increase in TL magnitude (across all frequencies) of the stacked structures compared to individual samples. The magnitude of the TL peak, however, was over-predicted by the FEA. This over-prediction was attributed to the exclusion of membrane damping from the FEA model.

Varying the stacking distance between the structures produced the greatest effect on TL at frequencies above the membrane resonance (3.4 kHz). The additional resonance observed at high frequency was a result of the mass–spring effect of the air space between the two layers. This mass–spring effect accounts for the dependence of the high-frequency resonance on stacking distance, with the air space behaving as the mass and the spring behavior resulting from the restoring force of each membrane. Symmetry of the stacked structures with respect to sample order was also observed for both the identical and non-identical structures.

Measurement of TL for arrays of LRAM with uniform mass distribution resulted in a single TL-peak profile (see Fig. 5) with frequencies similar to those predicted using FEA. Additionally, square single-celled structures provided direct comparison of TL performance to the four-celled array structure. The measured frequencies for the four-celled array were higher than those measured for the square single cell due to pressure coupling occurring downstream of the sample. A FEA-predicted pressure field was previously used to explain the discrepancy between the single-cell and array frequencies.[26] The predicted coupling resulted in an apparent increase in structural stiffness between adjacent cells in the array, thus increasing the measured resonance and TL peak frequencies. Additionally, the difference in overall TL between the square single-cell and array structures was attributed to the difference in cross-sectional area of the impedance tube occupied by the tube adaptor—the increased tube adaptor area for the single cell increased the TL magnitude. Finally, predicted behavior of the four-celled structure with decreased frame compliance showed a decrease in TL peak bandwidth of about 700 Hz. This decrease was attributed to a decrease in resonance frequency of the frame material as a result of decreased frame elastic modulus (see Ref. 26).

FEA-predicted TL of the four-celled array structure yielded low-frequency resonance and TL peak frequencies accurate to within 10% of measured values. The FEA model was also utilized to predict the high-frequency behavior, which could not be measured due to the frequency cutoff of the large diameter impedance tube (~2 kHz). Differences between the measured and predicted values were attributed in part to simplifications in the model, such as the use of the shell structure. Additional error was introduced by imperfections in the experimental setup, such as mounting of the mass off-center within cells. This mutual mistuning of cells could result in inaccurate measurement of the overall TL peak frequency. To minimize this source of error, alignment tools were used to mount each mass at the center of the cell.

To better understand the dynamic response of the multi-celled array, acceleration and pressure of the four-celled sample were measured using the laser vibrometer while cells were excited under discrete-frequency excitation.[15] The single TL peak profile indicated that the cells behaved in unison under broadband excitation. The sample examined was a four-celled array (27.4 mm cell size) with a rubber membrane material (0.176 mm thickness, tension of 1.6×10^5 Pa). Modulus, density, and Poisson's ratio of the rubber material were 8.0×10^5 Pa, 980 kg/m^3, and 0.48, respectively. The mass distribution was 0.48 g/cell. Samples were mounted in the impedance tube and excited using the impedance tube speaker (see schematic Fig. 8). The measured TL behavior for the rubber-membrane structure (single cell and four-celled array) is shown in Fig. 9(a). A laser vibrometer was used to measure the acceleration of the central mass of the structure under single frequency excitation (TL peak frequency at 166 Hz), and pressure was measured using the impedance tube microphones. Figure 9(b) shows the naming convention for the four-celled array, while Figs. 9(c)–9(f) show measured acceleration at the center of each cell as well as measured pressure across the sample.

Comparison of the pressure and acceleration signals showed clearly that the acceleration of each of the cells was out of phase with the incident sound pressure wave (also indicating that the cells were accelerating in phase with each other). Although pressure was measured at a single position downstream of the sample, the design of the impedance tube creates a plane wave incident upon the sample, and because of the normal incidence, it was assumed that the pressure was uniform across the entire surface.

The near-180° phase difference between the pressure and acceleration signals demonstrates the negative dynamic mass behavior of the center of each cell at the peak TL

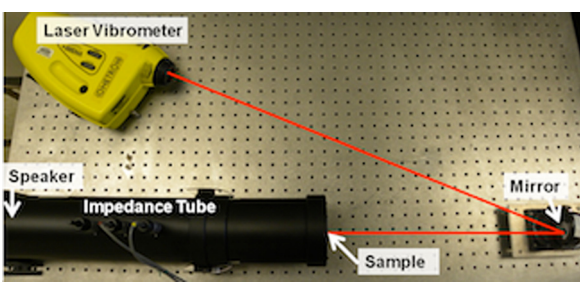

FIG. 8. (Color online) Schematic of measurement setup showing impedance tube, and laser vibrometer used for dynamic mass measurements.

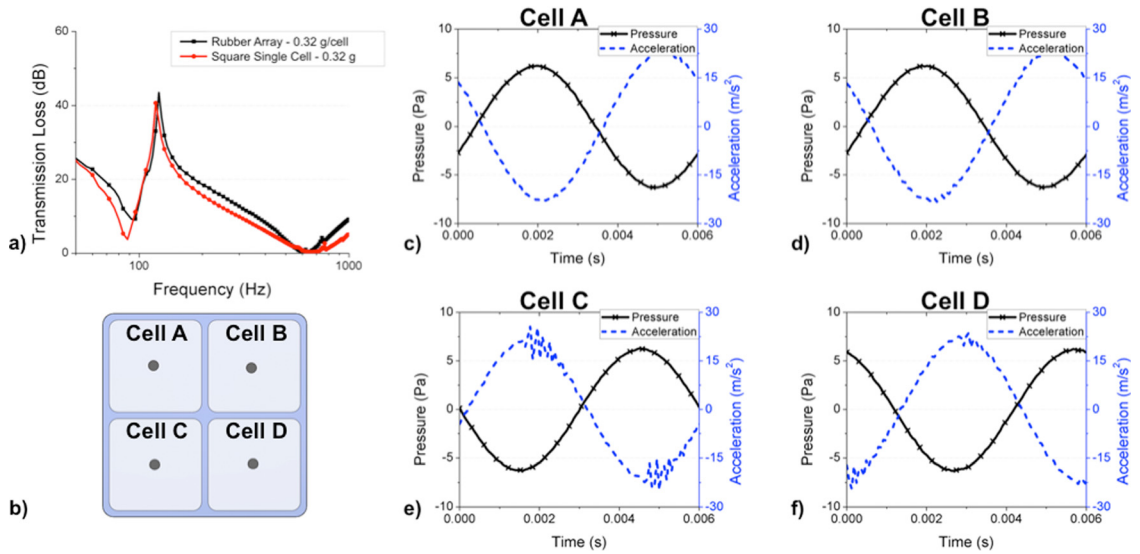

FIG. 9. (Color online) (a) Measured TL of four-cell and single-cell structures with rubber membrane, (b) schematic of four-celled structure, (c)–(f) measured acceleration and pressure amplitude as a function of time of each cell in the four-cell array. The mass distribution is 0.48 g/cell, and frequency is the TL peak frequency (rubber membrane, 166 Hz).

frequency. Negative dynamic mass, initially predicted using FEA by Yang *et al.*,[14] occurs when force and acceleration of the structure are opposite in sign. Negative dynamic mass is an effective property arising from the system dynamics of the structure. This behavior affects the TL performance because when the dynamic mass becomes negative, the wavenumber of the transmitted wave is imaginary, causing transmitted waves to decay exponentially rather than propagating into the far field. This decay of transmitted waves, in combination with the reflected sound waves resulting from the near-zero out-of-plane displacement,[14,15] resulted in overall increased TL.

Arranging the four-celled arrays in series resulted in either a single-peak or a multi-peak profile, depending on the mass distribution across each panel. Uniform mass distribution across both panels resulted in a single-peak profile with peak TL frequency ~19 dB greater than that of the single panel. This result was a significant increase over the acoustic mass law prediction of 6 dB TL increase when the surface density of a panel is increased by a factor of 2. The decay length of the transmitted waves for a single LRAM cell was calculated using Eq. (1) (see Yang *et al.*)[14] to be ~1.5 mm, where d was the decay length, r was the sample radius, f was the frequency, and c was the speed of sound in air,

$$d = \frac{\log 2}{\sqrt{\left(\frac{2\pi}{r}\right)^2 - \left(\frac{f}{c}\right)^2}}. \quad (1)$$

Due to this decay length compared to the separation distance between adjacent stacked panels, interaction between the panels was limited to a mass, air-spring effect typical of double-leaf panels. For this reason, stacking distance and stacking order did not affect the low-frequency TL peak behavior.

Previous studies[15,26] on membrane-type LRAM have examined both single-cell structures and arrays to understand the mechanism of sound insulation (in the first case), and to explore the interaction between cells and dynamics of the structure. Although these reports provided insights using both experimental and FEA techniques, the reports did not provide systematic analysis of scale-up behavior. Additionally, previous authors had presented experimentally measured results of stacked membrane-type LRAM, but had not included FEA-predicted response, or a thorough study including the effects of stacking distance and stacking order.

V. CONCLUSIONS

The acoustic behavior of three types of LRAM samples was investigated. Two simple structures—a single cell and a small-scale (four-celled) array—were evaluated and used to understand the acoustic response with changes in geometry and stacking of the structures in series. Systematic scale-up of the LRAM structure was performed with consistent results across both structure sizes reported and for the different geometric variations evaluated. The consistency of these results provides confidence in the ability to not only tune the acoustic performance of such simple small-scale structures, but to also design larger scale structures with the desired TL characteristics.

The practical significance of these findings remains partly unclear because of some of the outstanding challenges associated with large-scale structures that must be addressed. For example, the frame resonance frequency must be properly tuned to preserve the TL peak, and overall structural weight must be minimized when considering cell geometries. Employing thicker frames comprised of materials with reduced compliance is expected to increase the frame resonance frequency. To address structural weight of the LRAM, however, frame material should be minimized, as the largest contribution to overall weight comes from the frame material. By increasing cell size (thus decreasing the amount of frame material used), weight can be minimized. Geometric

variations, such as increase in mass diameter, increase in tension, or increase in membrane thickness, can then be implemented to tune the TL peak frequency to the desired range.

ACKNOWLEDGMENT

The authors would like to thank HRL Laboratories for support of this research.

[1]J. F. Wilby, "Aircraft interior noise," J. Sound Vib. **190**(3), 545–564 (1996).
[2]P. Wennhage, "Weight optimization of large scale sandwich structures with acoustic and mechanical constraints," J. Sandwich Struct. Mater. **5**, 253–266 (2003).
[3]S. Rajaram, T. Wang, and S. Nutt, "Small-scale transmission loss facility for flat lightweight panels," Noise Control Eng. J. **57**(5), 536–542 (2009).
[4]J. A. Moore and R. H Lyon, "Sound transmission loss characteristics of sandwich panel constrictions," J. Acoust. Soc. Am. **89**, 777–791 (1991).
[5]L. E. Kinsler, A. R. Frey, A. B. Coppens, and J. V. Sanders, *Fundamental of Acoustics*., 4th ed. (Wiley, New York, 2000), p. 163.
[6]K. Idrisi, M. E. Johnson, A. Toso, and J. P. Carneal, "Increase in transmission loss of a double panel system by addition of mass inclusions to a poro-elastic layer: A comparison between theory and experiment," J. Sound Vib. **323**, 51–66 (2009).
[7]C. J. Naify, C. Huang, M. Sneddon, and S. Nutt, "Transmission loss of honeycomb sandwich structures with attached gas layers," Appl. Acoust. **72**(2-3), 71–77 (2011).
[8]M. Dah-You, "Theory and design of microperforated panel sound-absorbing constructions," Sci. Sin. **18**(1), 55–71 (1974).
[9]V. G. Veselago, "The electrodynamics of substances with simultaneously negative values of ε and μ," Phys. Usp. **10**(4), 509 (1968).
[10]F. Bongard, H. Lissek, and J. R. Mosig, "Acoustic transmission line metamaterial with negative/zero/positive refractive index," Phys. Rev. B **82**, 094306 (2010).
[11]S. H. Lee, C. M. Park, Y. M. Seo, Z. G. Wang, and C. K. Kim, "Acoustic metamaterial with negative density," Phys. Lett. A **373**, 4464–4469 (2009).
[12]S. H. Lee, C. M. Park, Y. M. Seo, Z. G. Wang, and C. K. Kim, "Acoustic metamaterial with negative modulus," J. Phys.: Condens. Matter **21**(17), 175704 (2009).
[13]S. H. Lee, C. M. Park, Y. M. Seo, Z. G. Wang, and C. K. Kim, "Composite acoustic medium with simultaneously negative density and modulus," Phys. Rev. Lett. **104**, 054301 (2010).
[14]Z. Yang, J. Mei, M. Yang, N. H. Chan, and P. Sheng, "Membrane-type acoustic metamaterials with negative dynamic mass," Phys. Rev. Lett. **101**, 204301 (2008).
[15]C. J. Naify, C. M. Chang, G. McKnight, and S. Nutt, "Transmission loss and dynamic response of membrane-type locally resonant acoustic metamaterials," J. Appl. Phys. **108**(11), 114905 (2010).
[16]S. A. Cummer and D. Schurig, "One path to acoustic cloaking," New J. Phys. **9**(45), 45 (2007).
[17]M. D. Guild, A. Alu, and M. R. Haberman, "Cancellation of acoustic scattering from an elastic sphere," J. Acoust. Soc. Am. **129**(3), 1355–1365 (2011).
[18]A. N. Norris, "Acoustic cloaking theory," Proc. R. Soc. London, Ser. A **464**, 2411–2434 (2008).
[19]X. F. Li, X. Ni, L. Feng, M. H. Lu, C. He, and Y. F. Chen, "Tunable unidirectional sound propagation through a sonic-crystal-based acoustic diode," Phys. Rev. Lett. **106**, 084301 (2011).
[20]R. Martinez-Sala, J. Sancho, J. V. Sanches, V. Gomez, J. Llinares, and F. Meseguer, "Sound attenuation by sculpture," Nature (London) **378**(241), 241 (1995).
[21]J. V. Sanchez-Perez, D. Caballero, R. Martinez-Sala, C. Rubio, J. Sanchez-Dehesa, F. Meseguer, J. Llinares, and F. Galvez, "Sound attenuation by a two-dimensional array of rigid cylinders," Phys. Rev. Lett. **80**(4), 5325–5328 (1998).
[22]Z. Liu, X. Zhang, Y. Mao, Z. Yang, C. T. Chan, and P. Sheng, "Locally resonant sonic materials," Science **289**, 1734–1736 (2000).
[23]M. Hirsekorn, P. P. Delsanto, N. K. Batra, and P. Matic, "Modeling and simulation of acoustic wave propagation in locally resonant sonic materials," Ultrasonics **42**, 231–235 (2004).
[24]K. M. Ho, C. K. Cheng, Z. Yang, X. X. Zhang, and P. Sheng, "Broadband locally resonant sonic shields," Appl. Phys. Lett. **83**(26), 5566–5568 (2003).
[25]Z. Yang, H. M. Dai, N. H. Chan, G. C. Ma, and P. Sheng, "Acoustic metamaterial panels for sound insulation in the 50-1000 Hz regime," Appl. Phys. Lett. **96**, 041906 (2010).
[26]C. J. Naify, C. M. Chang, G. McKnight, F. Scheulen, and S. R. Nutt, "Membrane-type metamaterials: Transmission loss of multi-celled arrays," J. Appl. Phys. **109**, 104902 (2011).
[27]ASTM E2611-09: *Standard Test Method for Measurement of Normal Incidence Sound Transmission of Acoustical Materials Based on the Transfer Matrix Method* (American Standards for Testing and Materials, West Conshohocken, PA, 2009).
[28]D. T. Blackstock, *Fundamentals of Physical Acoustics*, 1st ed. (Wiley, New York, 2000), pp. 208–211.
[29]L. M. Brekhoviskikh and O. A. Godin, *Acoustics of Layered Media 1: Plane and Quasi-Plane waves* (Springer, Berlin, 1990), p. 31.
[30]L. L. Beranek and I. L. Ver, *Noise and Vibration Control Engineering*, 2nd ed. (Wiley, New York, 1992), p. 219.